Article

Spectral Diffusion Induced by Proton Dynamics in Pigment#Protein Complexes

Marc Brecht, Hauke Studier, Volker Radics, Jana B. Nieder, and Robert Bittl

J. Am. Chem. Soc., **2008**, 130 (51), 17487-17493 • DOI: 10.1021/ja806216p • Publication Date (Web): 03 December 2008

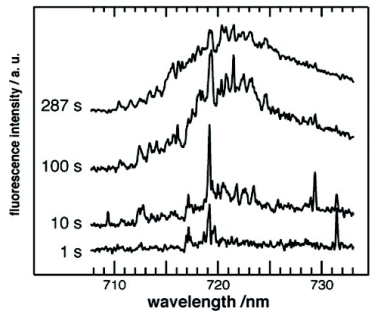

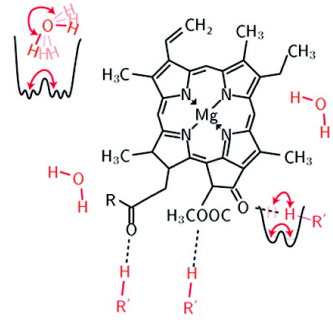

More About This Article

Additional resources and features associated with this article are available within the HTML version:

- Supporting Information
- Access to high resolution figures
- Links to articles and content related to this article
- Copyright permission to reproduce figures and/or text from this article

View the Full Text HTML

J|A|C|S
ARTICLES

Published on Web 12/03/2008

Spectral Diffusion Induced by Proton Dynamics in Pigment−Protein Complexes

Marc Brecht,* Hauke Studier, Volker Radics, Jana B. Nieder, and Robert Bittl

Fachbereich Physik, Freie Universität Berlin, Arnimalle 14, 14195 Berlin, Germany

Received August 7, 2008; E-mail: marc.brecht@physik.fu-berlin.de

Abstract: The fluorescence emission of individual photosystem I complexes from *Synechocystis* PCC 6803 in protonated and deuterated buffer shows zero-phonon lines as well as broad intensity distributions. The number and the line width of the zero phonon lines depend strongly on the solvent (H_2O/D_2O). The spectral diffusion rate of the whole fluorescence emission from photosystem I is significantly reduced upon deuteration of the solvent. This leads to a substantial increase of well-resolved zero-phonon lines. Since the chlorophyll a chromophores lack exchangeable protons, these observed changes in the spectral diffusion have to be assigned to exchangeable protons at the amino acids and structural water molecules in the chromophore binding pocket.

Introduction

Single-molecule techniques offer a unique tool for studying the dynamical behavior of molecules. They provide the possibility to observe individual processes in real time and enable one to reconstruct distributions from single events and reassemble ensemble signals from bottom up.[1] Applying single-molecule experiments on proteins has revealed new insights, like the observation of fluctuations in the rates of enzyme catalysis as well as large fluctuations of the transition energy of chromophores.[2−4] The observed effects are interpreted in terms of fluctuations of the protein (enzyme) between various conformational substates.[5]

The dynamics between the conformational substates is an inherent property of all proteins. It happens on multiple time scales from tens of femtoseconds to hundreds of seconds.[6] Each motional mode in proteins is associated with a typical time scale, for example, local vibrations happen within hundreds of femtoseconds and large scale motions, such as domain movements, occur in milliseconds to seconds.[6]

Conformational dynamics occurs on a complex, rugged energy landscape characterized by a large number of different conformational substates, as shown by the pioneering experiments of Frauenfelder and co-workers on myoglobin.[7] The conformational substates correspond to local minima in the potential energy surface. Protein energy landscapes are characterized by the existence of many, nearly isoenergetic, local minima, which are organized in a hierarchical structure.

The hierarchical organization of the energy landscape was demonstrated in single-molecule experiments on light-harvesting complexes[8] where different absorption properties of individual chromophores were found as well as a dynamical hopping between conformational substates of single chromophores. These experiments are based on the fact that changes between conformational substates of a protein induce changes in the site-energy of a chromophore and thus in its absorption and emission wavelength. The largest influence on the site-energy occurs for conformational variations of the chromophore itself and/or its close surrounding.[8] The observed spectral hopping of lines in single-molecule experiments often relies on the higher barrier crossing probability between conformational substates in the excited-state of the chromophore than in the ground state.[9] These activated barrier crossings enable single chromophores to map the energy landscape even at low temperatures and thus provide a spectroscopic tool to obtain general insights into the characteristics of protein energy landscapes.

With single-molecule techniques at low temperature, where large scale motions of the protein are frozen out, these changes of the site-energy can be directly observed. Despite the reduced conformational dynamics at low temperatures, the observed changes in the site-energy reach into the nm range.[10,11] An assignment of the origin of the observed changes in the site-energy is still missing, and this study focuses on the physical origin of the site-energy variations.

Fluctuations of the site-energy are observed here by single-molecule experiments on Photosystem I (PSI). The favorable spectroscopic properties of PSI for these experiments are

(1) Tamarat, P.; Maali, A.; Lounis, B.; Orrit, M. *J. Phys. Chem. A* **2000**, *104*, 1–16.
(2) Tinnefeld, P.; Sauer, M. *Angew. Chem., Int. Ed.* **2005**, *44*, 2642–2671.
(3) Schuler, B. *ChemPhysChem* **2005**, *6*, 1206–1220.
(4) Moerner, W. E. *Proc. Natl. Acad. Sci. U.S.A.* **2007**, *104*, 12596–12602.
(5) Flomenbom, O.; Velonia, K.; Loos, D.; Masuo, S.; Cotlet, M.; Engelborghs, Y.; Hofkens, J.; Rowan, A. E.; Nolte, R. J. M.; Van der Auweraer, M.; de Schryver, F. C.; Klafter, J. *Proc. Natl. Acad. Sci. U.S.A.* **2005**, *102*, 2368–2372.
(6) Zwanzig, R. *Acc. Chem. Res.* **1990**, *23*, 148–152.
(7) Austin, R. H.; Beeson, K. W.; Eisenstein, L.; Fraunefelder, H.; Gunsalus, I. C. *Biochemistry* **1975**, *14*, 5355–5373.
(8) Hofmann, C.; Aartsma, T. J.; Michel, H.; Kohler, J. *Proc. Natl. Acad. Sci. U.S.A.* **2003**, *100*, 15534–15538.
(9) Jankowiak, R.; Hayes, J. M.; Small, G. *J. Chem. Rev.* **1993**, *93*, 1471–1502.
(10) Hofmann, C.; Michel, H.; van Heel, M.; Kohler, J. *Phys. Rev. Lett.* **2005**, *94*, 195501.
(11) de Ruijter, W. P. F.; Segura, J. M.; Cogdell, R. J.; Gardiner, A. T.; Oellerich, S.; Aartsma, T. *J. Chem. Phys.* **2007**, *341*, 320–325.

summarized shortly.[12−14] PSI harbors a large number of chlorophyll a (Chla) molecules (∼100 Chla per PSI monomer) involved in light harvesting, exciton transfer, and charge separation.[15] A species-dependent number of Chla molecules shows a remarkably red-shifted absorption/fluorescence. These Chla-species are often called the "red-pools" or "red-most" Chla's (for a review see, e.g., ref 16, 17). At low temperatures these red-shifted Chla's function as traps for a large fraction of the captured excitation energy by the antenna system. The trapped energy is then partially released by fluorescence emission. The large antenna system together with the effective exciton transfer network allows a very efficient excitation of PSI at the maximum of its absorption (∼680 nm) far from the maximum of the fluorescence emission (∼730 nm). Because of this advantage, the whole fluorescence emission of PSI can be observed without interference by the excitation light down to the single-molecule level.

The fluorescence emission of PSI from *Synechocystis* PCC 6803 consists of several contributions that differ in their spectroscopic properties like emission wavelength, intensity, electron−phonon coupling, and the degree of spectral diffusion.[13,14,18−21] The extensively studied spectroscopic properties of PSI as well as the availability of the well-resolved structural model make PSI an excellent choice for studies of protein-cofactor interactions.

Material and Methods

PSI from *Synechocystis* PCC 6803 has been isolated and prepared as described in ref 21, 22. For H/D exchange, samples of purified PSI trimers were at first diluted in deuterated buffer at pD 7.66 containing 20 mM Tricine, 25 mM $MgCl_2$, and 0.4 mM (0.02% w/v) detergent (β -DM, Sigma), to reach a concentration of about 20 μM Chla. This amount of detergent is adequate to avoid aggregation of PSI trimers.[23] For prereduction of P700 5 mM Na-ascorbate was added. In further steps this PSI containing solution was diluted to a PSI trimer concentration of 3 pM. Less than 1 μL of this sample was placed between two coverslips, assuring spatial separation of individual PSI trimers. Sample preparation and mounting were accomplished under indirect daylight. The experiments were carried out in a laboratory-built confocal microscope as described in ref 13 at a temperature of 1.4 K.

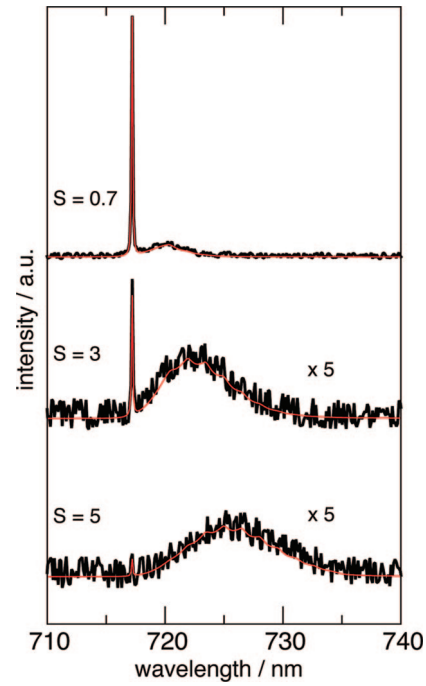

Figure 1. Simulations of the line shape as a function of the strength of the electron−phonon coupling using the expression given in ref 33. The Huang−Rhys factor S was changed as indicated in the plots (red curves). A noise level comparable to the experimental situation (for a spectrum taken within 1 s) was added, while the integrated intensity of the whole emission line (ZPL and PW) was kept constant (black curves). Parameters: Width of the ZPL, $\Delta\lambda_{ZPL} = 2$ cm^{-1}; mean frequency for the phonon-distribution, $\omega = 30$ cm^{-1}; width of the phonon-distribution, $\Delta\omega = 30$ cm^{-1}.

Results

Emission Spectra of Individual Complexes. In the low temperature limit the shape of a single emitting species in the condensed phase consists of a narrow zero-phonon-line (ZPL) and a broad phonon wing (PW).[9] The ZPL belongs to a pure electronic transition without phonon (lattice vibrational mode) creation or annihilation. The PW on the low energy side of the ZPL is due to the interaction of the chromophore with its surrounding, leading to the excitation of phonons at the expense of the photon energy. The intensity distribution between the ZPL and PW is given by $e^{-S} = I_{ZPL}/(I_{ZPL} + I_{PW})$, with the Huang−Rhys factor S,[24] a quantity closely related to the Debye−Waller factor. The resulting line shapes using different S-values are shown by simulations in Figure 1 under the assumption of typical signal-to-noise ratios in our experiments.

The experiments on the single-molecule level were carried out on PSI from *Synechocystis* PCC 6803 showing three contributions F699, C706 (also referred to as C708[20]), and C714 to the fluorescence at low temperature.[19,21,25] The abbreviations originate from an emission maximum at 699 nm[21] and two absorption maxima at 706 and 714 nm,[26] respectively. Figure 2 shows fluorescence emission spectra (denoted I−V) of single

(12) Jelezko, F.; Tietz, C.; Gerken, U.; Wrachtrup, J.; Bittl, R. *J. Phys. Chem. B* **2000**, *104*, 8093–8096.
(13) Brecht, M.; Studier, H.; Elli, A. F.; Jelezko, F.; Bittl, R. *Biochemistry* **2007**, *46*, 799–806.
(14) Brecht, M.; Nieder, J. B.; Studier, H.; Schlodder, E.; Bittl, R. *Photosynth. Res.* **2008**, *95*, 155–162.
(15) Jordan, P.; Fromme, P.; Witt, H. T.; Klukas, O.; Saenger, W.; Krauss, N. *Nature* **2001**, *411*, 909–917.
(16) Gobets, B.; van Grondelle, R. *Biochim. Biophys. Acta, Bioenerg.* **2001**, *1507*, 80–99.
(17) Karapetyan, N. V.; Schlodder, E.; van Grondelle, R.; Dekker, J. P. Photosystem I: The Light-Driven Plastocyanin:Ferredoxin Oxidoreductase. *Advances in Photosynthesis and Respiration*; Springer, New York, 2007; Vol. 24.
(18) Ratsep, M.; Johnson, T. W.; Chitnis, P. R.; Small, G. J. *J. Phys. Chem. B* **2000**, *104*, 836–847.
(19) Zazubovich, V.; Matsuzaki, S.; Johnson, T. W.; Hayes, J. M.; Chitnis, P. R.; Small, G. *J. Chem. Phys.* **2002**, *275*, 47–59.
(20) Hsin, T. M.; Zazubovich, V.; Hayes, J. M.; Small, G. J. *J. Phys. Chem. B* **2004**, *108*, 10515–10521.
(21) Brecht, M.; Radics, V.; Nieder, J. B.; Studier, H.; Bittl, R. *Biochemistry* **2008**, *47*, 5536–5543.
(22) Bautista, J. A.; Rappaport, F.; Guergova-Kuras, M.; Cohen, R. O.; Golbeck, J. H.; Wang, J. Y.; Beal, D.; Diner, B. A. *J. Biol. Chem.* **2005**, *280*, 20030–20041.
(23) Müh, F.; Zouni, A. *Biochim. Biophys. Acta, Bioenerg.* **2005**, *1708*, 219–228.
(24) Huang, K.; Rhys, A. *Proc. R. Soc. London, Ser, A* **1950**, *204*, 406–423.
(25) Gobets, B.; van Amerongen, H.; Monshouwer, R.; Kruip, J.; Rogner, M.; van Grondelle, R.; Dekker, J. P. *Biochim. Biophys. Acta, Bioenerg.* **1994**, *1188*, 75–85.
(26) Riley, K. J.; Reinot, T.; Jankowiak, R.; Fromme, P.; Zazubovich, V. *J. Phys. Chem. B* **2007**, *111*, 286–292.

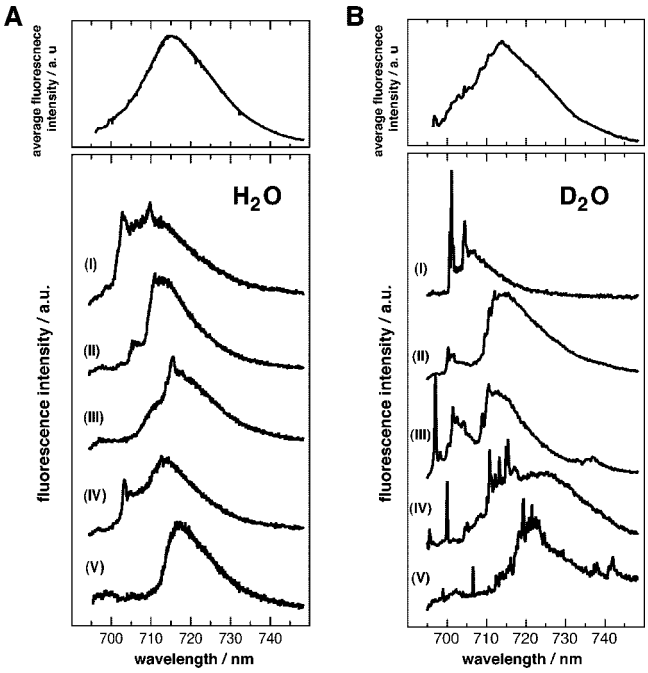

Figure 2. Single-molecule fluorescence emission spectra from different PSI complexes of *Synechocystis* PCC 6803 in (A) H_2O- and (B) D_2O-based buffer. Excitation was at 680 nm, and the accumulation time was 100 s for each complex. Panel tops show average spectra of all studied complexes (100 complexes in H_2O buffer, 60 complexes in D_2O buffer).

PSI complexes in (A) H_2O- and (B) D_2O-based buffer. The acquisition time for each spectrum was 100 s. For better comparability, the spectra were scaled to a similar magnitude. The spectra shown in panel A are adapted from ref 21 and were described in detail there. The spectra taken in D_2O buffer show more resolved ZPLs, and their line widths are smaller than in H_2O buffer while the same overall shapes of spectra are observed in both cases. Furthermore, the spectra taken in D_2O buffer show ZPLs in the wavelength range larger than 720 nm where almost no lines were observed in the H_2O case. The increased number of observed ZPLs and their smaller line width indicate a slower spectral diffusion in D_2O buffer compared to H_2O buffer. On top of the spectra from single complexes the average spectra obtained from the summation of the fluorescence emission spectra of all studied PSI complexes in H_2O (100) and D_2O (60) are given. Both spectra agree well with bulk emission spectra. The only significant difference between the spectra is the rather smooth shape of the average spectrum of the 100 complexes in the case of H_2O buffer, while the spectrum for the 60 complexes in D_2O buffer still shows residual narrow structures. This difference cannot be attributed to the different numbers of observed complexes but originates from the difference in the number and width of resolved ZPLs in the two buffers.

ZPLs Show Dynamical Variations of Their Spectral Position and Intensity. Electronic energy level fluctuations of the protein-embedded pigments can be monitored directly as line jumps or indirectly as line broadening. Observation of line jumps is possible if the fluctuations are slow compared to the experimental time resolution, whereas line broadening is observed in cases when the fluctuations are faster than the time resolution of the experiment.[11,27] Therefore, the underlying dynamical processes leading to the spectral broadening can be resolved by reducing the accumulation time for the spectra. Spectra with sufficient signal-to-noise ratio can be taken with ~1 s acquisition time in our setup. Sequences of the complete fluorescence emission spectra were taken in order to analyze the spectral dynamics. In the following we focus on the dynamical behavior of some ZPLs within these spectra. Therefore, only the wavelength region of interest will be shown. Two sequences showing representative examples of the dynamical behavior of ZPLs are given in Figures 3 and 4.

Figure 3 shows a sequence of 200 spectra taken with 1 s acquisition time for each spectrum. The spectrum on top represents the sum of these 200 spectra. The picture shows the time dependent movement of two ZPLs, one in the region between 700−706 nm and the other in the region between 710−715 nm, both regions are indicated by white dotted lines. The ZPL in the region 700−706 nm shows only few large frequency jumps (for example in the first 20 s), but otherwise shows emission almost stable at a wavelength ~701 nm. The spectral trail of the ZPL in the range 710−715 nm shows more jumps with variable jump widths. This ZPL is accompanied by an intense PW. The spectral shape of the ZPL and its PW remains unchanged during the significant jumps of the ZPL position over several nm, as shown for three different wavelength positions in Figure 3B. The shape stability of the emission line irrespective of the particular line position allows the extraction of the Huang−Rhys factor for this emitter after appropriate shifting of the line for signal-to-noise enhancement as shown in Figure 3C trace c1. Numerical integration of the intensities of the sharp ZPL (709.8−710.8) and the PW (710.8−730 nm; width given by the horizontal bar below trace c1) yields $S = 2.9 \pm 0.5$. This value indicates a strong coupling of the involved chromophores with the environment.[18]

For the line in the 700−706 nm range a PW is harder to detect. During the interval from 15−17 s the ZPL remains within a very narrow wavelength interval and the PW can be identified in the spectrum averaged over this interval as shown in Figure 3C trace c2. Using the numerically integrated intensity of the ZPL (700.3−701.3 nm) and the PW (701.3−705.5 nm; see horizontal bar below trace c2) yields a Huang−Rhys factor of $S = 0.53 \pm 0.05$ indicating a weak coupling of the chromophore to its environment.[18,20]

A second example for the dynamic behavior of ZPLs is given by the sequence shown in Figure 4. The spectrum on top represents the average of all spectra, and the graph on the right shows the time dependence of the integrated intensity of the spectra. The mean position of the emitted intensity shows a wavelike motion during the 287 s of accumulation. At the beginning the mean position of the trail is centered around 720 nm, from there it moves within the following 100 s toward 725 nm. Then it moves in the time period from 100−200 s to around 715 nm and from there back again to the red. The variation of the mean position during time is mirrored by a similar variation of the integrated intensity (graph on the right of the sequence). We observe reduced intensity if the spectral mean position is on the red side and increased intensity if it is on the blue side. The correlation coefficient between the mean position and the intensity is 0.65.

The individual spectra of this sequence are dominated by strong ZPLs. Some spectra show one ZPL, but mostly more than one line is visible. As examples, four spectra out of this sequence are shown in Figure 4B. The number of lines as well as their spectral positions differ. The spectra taken at 68 and

(27) Rutkauskas, D.; Novoderezhkin, V.; Cogdell, R. J.; van Grondelle, R. *Biophys. J.* **2005**, *88*, 422–435.

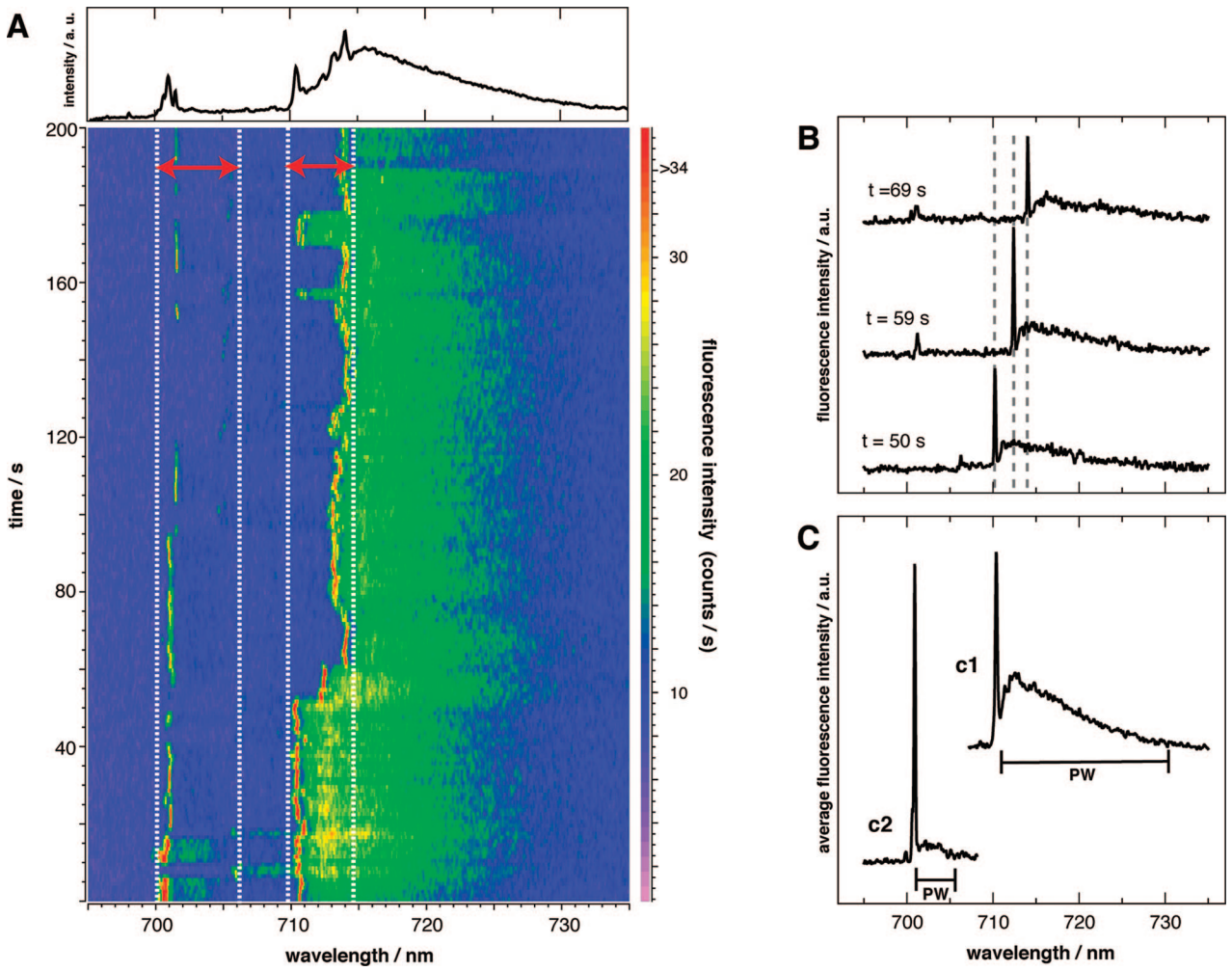

Figure 3. (A) Sequence of 200 fluorescence spectra taken continuously on one single complex. The acquisition time of the single spectra was 1 s. The summation of all spectra is given on top of the sequence. White dashed lines indicated the regions wherein the ZPLs reside. (B) Three single spectra out of the sequence given in A. (C) For the determination of the Huang−Rhys factor of the emitter in the range 710−715 nm, 16 spectra where the ZPL resides almost on the same position (here 710.4 nm) were summed up (c1), the assumed width of the PW (710.8−730 nm) is given by a bar. For the ZPL in the range 700−706 nm the spectra between 15−17 s were summed up (c2), the assumed width of the PW (from 701.3−705.5 nm) is indicated by a bar, for more details see also the text.

113 s show three ZPLs, the spectrum at 180 s shows just one line. In the spectrum at 192 s at minimum eight lines are discernible. The intensity of the ZPLs show the tendency to decrease if a larger number of ZPLs are observed within one spectrum. This observation suggests one emitter as common origin for these ZPLs.

Integration of spectra from the recorded sequences is equivalent to increasing the accumulation time of an individual spectrum. Such integrations are given in Figure 4C for 10 s, 100 s, and for the whole sequence (287 s). These spectra show the transition from spectra dominated by resolved lines (1 and 10 s) to inhomogeneously broadened spectra (100 and 287 s) that are usually observed in samples in H_2O buffer also for short acquisition times.

Heterogeneity of the Spectral Positions of ZPLs and Their Number. As it can be seen in the spectra shown in Figure 3 and 4, the dynamic behavior of the ZPLs is heterogeneous. The heterogeneity concerns not only the dynamic behavior between individual complexes, but also the dynamics within one complex. Despite this heterogeneity, we observe, as a common feature, that the ZPLs remain in restricted spectral areas. The borders of such areas are visualized by white dotted lines in Figures 3 and 4. Those areas were determined from time-dependent spectra sequences of 60 individual PSI complexes in deuterated buffer to obtain an overview of their spectral positions and widths. The areas collected are given in Figure 5A. The spectral ranges occupied by the spectral trails of ZPLs are in some cases well separated and in others they overlap. If the spectral trails are well separated, the bars represent the dynamic region of one single line. In the case of overlapping ranges, the ranges were combined and are given as one joint bar. Therefore, a direct correlation of the width of a bar with the spectral band covered by an individual line is not possible. As it can be seen in Figure 5A the extension and number of the spectral ranges covered by ZPLs vary from complex to complex.

Horizontal cuts through the chart in Figure 5A yield the probability of finding ZPLs at a specific wavelength. These probabilities are shown in Figure 5B for 1 nm wide wavelength intervals. In the range 695−715 nm the probability remains almost constant on a high level, followed by a steep decay within the wavelength range 715−725 nm; then the curve decays smoothly. For comparison, the corresponding curve for PSI from *Synechocystis* PCC 6803 in H_2O buffer from ref 14 is included in the figure. It shows an almost monotonous decay from 697

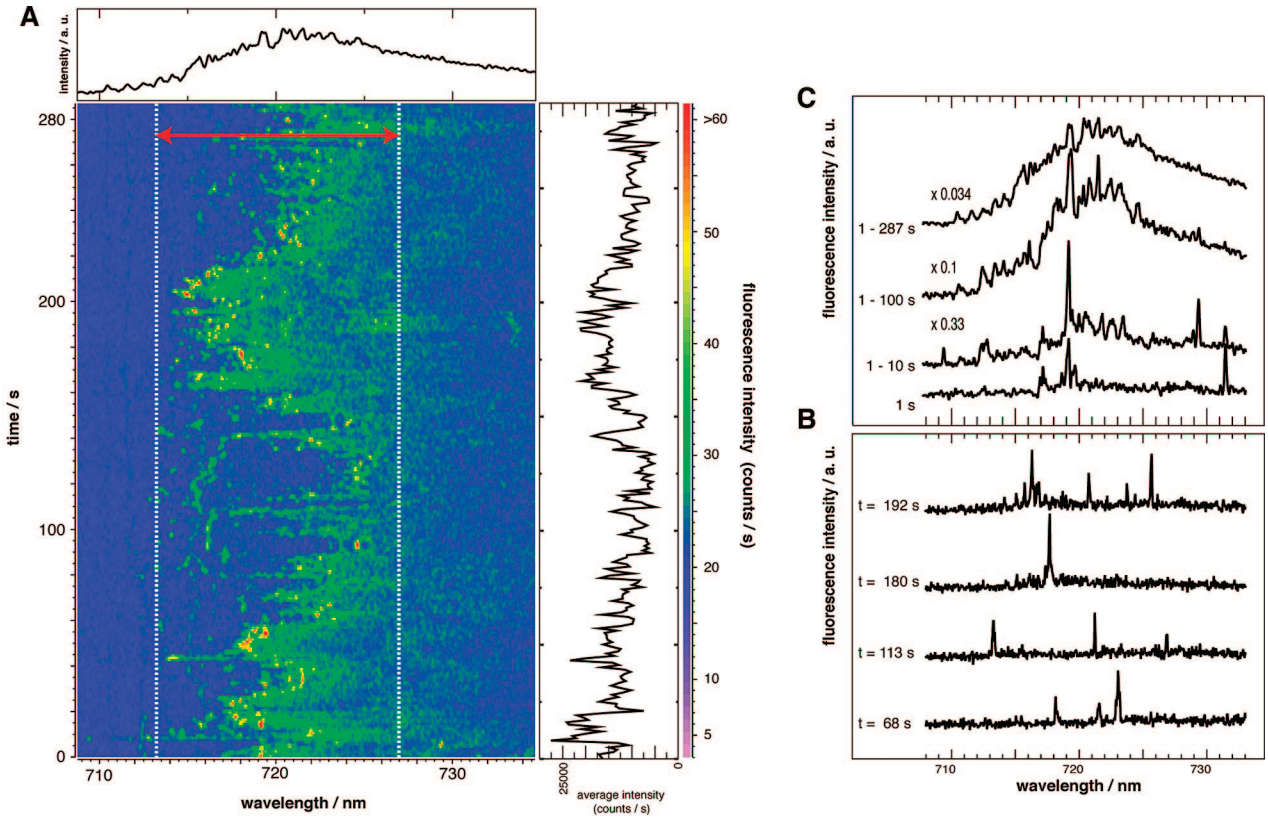

Figure 4. (A) Sequence of 287 fluorescence spectra taken continuously on one single complex. The acquisition time of the single spectra was 1 s. The summation of all spectra is given on top of the sequence. The integrated intensity of the single spectra over time is given on the right side. White dashed lines indicate the region (713−727 nm) wherein the ZPLs reside. (B) Four single spectra out of the sequence. The ZPL positions are 718.2, 721.6, and 723.1 nm (t = 68 s), 713.3, 721.3, and 726.9 nm (t = 113 s), 717.8 nm (t = 180 s). The spectrum at t = 192 s shows at minimum eight ZPLs, the three most intense lines are at 716.3, 720.8, and 725.7 nm. (C) Visualization of the broadening effect by increasing the accumulation time, the first spectrum of the sequence (t = 1 s) as well as the summation of the spectra from 1−10, 1−100, and 1−287 s are given; these spectra were scaled and smoothed.

to 722 nm. The observation of ZPLs at wavelengths larger than 722 nm remains an exception in H_2O. The difference between the probability of observing ZPLs in the deuterated and the protonated sample given in Figure 5C shows a broad distribution with its center close to 714 nm. Additionally, a Gaussian line is included with its maximum position and line width given for C706 (red curve) in ref 19.

Discussion

Effect of D_2O As Solvent on Spectra of Single PSI Complexes. The average emission spectra of single PSI complexes from *Synechocystis* PCC 6803 in deuterated and protonated buffer are in good agreement with the reported bulk emission spectra.[18,25] The inhomogeneous broadening dominating the bulk emission can be lifted by single-molecule spectroscopy (SMS), and the fluorescence emission of single complexes can be observed (Figure 2). The single-molecule spectra from *Synechocystis* PCC 6803 exhibit a distinct heterogeneity, but they share general features like broad intensity distributions and ZPLs. The spectral position and the intensity of the observed features vary from complex to complex. The number of ZPLs observed in deuterated buffer exceeds the number of ZPLs observed in protonated buffer and the line width of the ZPLs remains smaller in deuterated than in protonated buffer. All pools contributing to the PSI emission in complexes from *Synechocystis* PCC 6803 (F699, C706, and C714) are affected and, therefore, are accessible by the solvent (water) molecules.

Besides the ZPLs, broad intensity distributions are observed in the single-molecule spectra. Comparable broad distributions were found for PSI from *Thermosynechoccocus elongatus*[13] and *Synechococcus* PCC 7002[14] as well as for the light harvesting complexes LH2 and LH3.[11] It was argued that these broad intensity distributions are built up by fast diffusing ZPLs.[11,13] This assumption is clearly corroborated here by the findings shown in Figure 4 for PSI complexes in D_2O buffer. Individual emission spectra recorded on the 1 s time scale show well-resolved lines. Increasing the acquisition time or numerically integrating over sequences of time-resolved spectra results in unstructured broad spectra. This is in good agreement with ensemble data and single molecule spectra acquired from PSI in H_2O buffer.

The direct observation of the assembly of broad unresolved spectra from individual well-resolved spectra dominated by ZPLs is due to altered spectral dynamics in D_2O buffer compared to H_2O. The rates of spectral diffusion changes, but the spectral width wherein the lines diffuse remains unchanged. Therefore, the changes in the site-energy remain similar upon H_2O to D_2O buffer exchange, but the time constants for the underlying conformational dynamics are affected.

This change in the spectral diffusion results in the difference of the ZPL probability, seen in Figure 5C. The most important difference occurs at long wavelengths, where in the case of H_2O buffer detection of resolved ZPLs is scarce. Because of the reduced spectral diffusion in D_2O buffer, the probability for

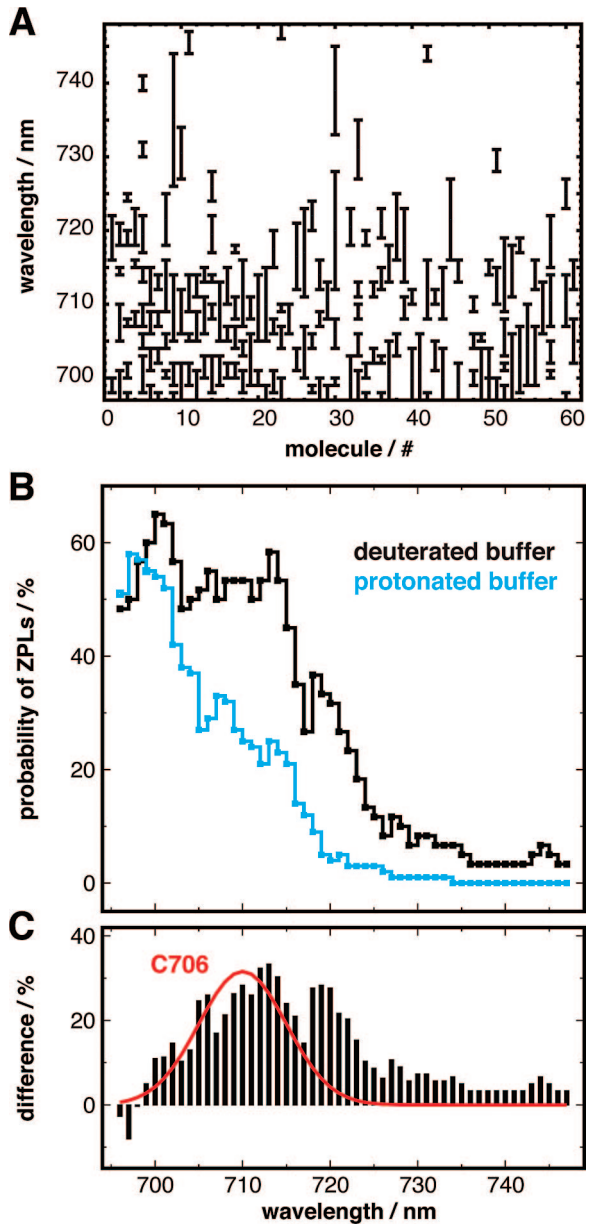

Figure 5. (A) Statistical analysis of the ZPL distribution. The chart shows the individual regions in which the ZPLs were observed in the sequences of spectra of 60 individual PSI complexes in D_2O buffer. The determination of these areas from the sequences is explained in the text and visualized in Figure 3 and 4. The average width of the regions is about 4.3 nm. (B) Horizontal cuts through the chart (A) give the probability of finding ZPLs at a specific wavelength, the bin size was 1 nm. For comparison the curve found for complexes in H_2O buffer from ref 14 is included (light blue curve). (C) Differences of the two curves are given in panel B. Additionally, a Gaussian line is included using the maximum position and the line width for C706 (red curve) given in ref 19.

ZPLs increases under identical experimental time resolution. A calculated emission profile for the C706 pool[19] using literature values for the spectral position and width resembles well the additional ZPL probability in D_2O buffer in the range below 715 nm. Therefore, we assign these ZPLs to the C706 pool. The remaining ZPLs beyond 717 nm can be assigned to the C714 pool.

Exchangeable Hydrogens As Origin of the Observed Spectral Diffusion. The conformational changes in a protein can be described in the model of a hierarchical energy landscape.[7]

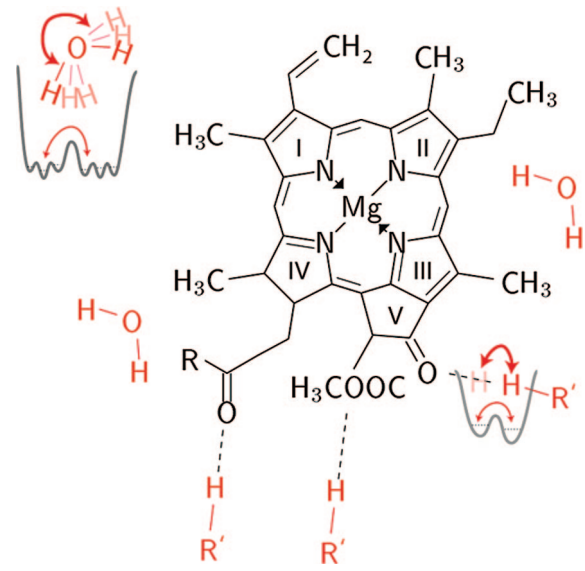

Figure 6. Schematic structure of Chla. Chla harbors two sites accessible for hydrogen bonds (the methyl-ester carbonyls and keto-group of ring *V*). These positions might be involved in hydrogen-bridges with potential partners in their close environment. Possible conformational motion in a TLS or *n*-TLS is illustrated.

Large conformational changes are due to changes of the substate in the first hierarchical tier, whereas smaller changes are due to conformational changes in the hierarchical levels below. The observed changes of the transition energy in the nm-range at cryogenic temperatures are believed to originate from conformational changes in the second tier.[8] These changes of the transition energy are due to changes in the chromophore itself or its surrounding. The influence of the surrounding decreases strongly with the distance, therefore, only fluctuations in the first coordination sphere of the chromophores must be taken into account.[28]

Our experiments show that the fluctuation rate between those substates is strongly determined by exchangeable hydrogens. The conformational fluctuation of these hydrogens affects the conjugated π-system of the macrocycle and yields the observed line jumps. Proton mobility in proteins is a prerequisite for function (for review see 29), and they are mobile even at helium temperatures.[30]

The Chla molecule harbors no bound hydrogens exchangeable at physiological pH conditions. Therefore interactions, like hydrogen bonds, between the Chla moiety and nearby amino acid residues as well as internal water molecules have to be taken into account.[8,31] Chla harbors two sites accessible for hydrogen bonds, these are the methyl-ester carbonyls and keto-group of ring *V*[32] (see also Figure 6). Ring *V* shows a large effect on its polarizability as a function of changes close to its keto-group[32] indicating a high sensitivity of the site-energy toward changes close to this keto-group. Fluctuations of a

(28) Lesch, H.; Schlichter, J.; Friedrich, J.; Vanderkooi, J. M. *Biophys. J.* **2004**, *86*, 467–472.
(29) Nagel, Z. D.; Klinman, J. P. *Chem. Rev.* **2006**, *106*, 3095–3118.
(30) Davydov, R.; Chemerisov, S.; Werst, D. E.; Rajh, T.; Matsui, T.; Ikeda-Saito, M.; Hoffman, B. M. *J. Am. Chem. Soc.* **2004**, *126*, 15960–15961.
(31) Helms, V. *ChemPhysChem* **2007**, *8*, 23–33.
(32) Shipman, L. L.; Janson, T. R.; Ray, G. J.; Katz, J. *J. Proc. Natl. Acad. Sci. U.S.A.* **1975**, *72*, 2873–2876.
(33) Pieper, J.; Voigt, J.; Renger, G.; Small, G. *J. Chem. Phys. Lett.* **1999**, *310*, 296–302.

hydrogen atom in H-bonds between the keto-groups and nearby amino acid residues or water molecules may induce the largest changes of the site-energy possible at cryogenic temperatures. The large number of wavelength positions accessible for the individual emitters in PSI implies that a simple two-level system (TLS) model, as used for visualization in Figure 6, is not capable of explaining the conformational dynamics of the H-bonds relevant for the spectral dynamics in PSI.

In summary, the observed spectral dynamics of single PSI complexes is strongly reduced in its rate by the exchange of the solvent from H_2O to D_2O. All red-pools contributing to the fluorescence emission are affected and therefore are accessible by the solvent. The structural origin of the spectral diffusion is most probable due to fluctuations of hydrogen atoms in the close environment of the conjugated π-system of the macrocycle of the emitting Chlas. The largest changes of the site-energy are suggested to stem from fluctuations of hydrogen atoms in an H-bond between the keto-group of ring *V* of the Chla and nearby amino acid residues or flucuations of internal water molecules.

Acknowledgement: We thank Eberhard Schlodder for helpful discussion. This work was supported by VolkswagenStiftung in the framework of the program Physics, Chemistry and Biology with Single Molecules (I/78361).

JA806216P